JOURNAL OF APPLIED ELECTROCHEMISTRY **18** (1988) 504–510

A consideration of circulating bed electrodes for the recovery of metal from dilute solutions

K. SCOTT

Department of Chemical Engineering, Teesside Polytechnic, Borough Road, Middlesbrough, Cleveland, UK

Received 31 March 1987; revised 10 November 1987

A comparison is made of three types of circulating particulate electrodes: spouted (circulating) bed (SBE), vortex bed (VBE) and moving bed (MBE). In applications such as metal recovery, all electrodes perform similarly in terms of current efficiency. On the basis of scale-up, it appears that the spouted bed electrode is the preferred system.

Nomenclature

I	cell current (A)
F	Faraday constant (94 487 $\mathrm{C\,mol^{-1}}$)
C	dimensionless concentration
C_F	friction factor
C_0	Initial concentration ($\mathrm{mol\,m^{-3}}$)
D	pipe equivalent diameter (m)
e_b	bed voidage
e_c	voidage of conveying section
L	bed length (m)
S_b	cross section area of bed ($\mathrm{m^2}$)
S_T	cross section area of conveying section ($\mathrm{m^2}$)
T	dimensionless time $= It/nFVC_0$
U_f	superficial liquid velocity in conveying ($\mathrm{m\,s^{-1}}$)
U_i	particle terminal velocity corrected for wall effects ($\mathrm{m\,s^{-1}}$)
U_s	particle velocity in transport ($\mathrm{m\,s^{-1}}$)
U_{SL}	slip velocity ($\mathrm{m\,s^{-1}}$)
t	time (s)
V	electrolyte volume ($\mathrm{m^3}$)
V_f	liquid velocity in the bed ($\mathrm{m\,s^{-1}}$)
V_{mf}	minimum fluidization velocity ($\mathrm{m\,s^{-1}}$)
V_s	particle velocity in the bed ($\mathrm{m\,s^{-1}}$)
ΔP	pressure drop ($\mathrm{NM^{-2}}$)
ϱ	fluid density ($\mathrm{kg\,m^{-3}}$)
ϱ_s	particle density ($\mathrm{kg\,m^{-3}}$)
Re	Reynolds number

1. Introduction

The early research on fluidized bed electrodes by, amongst others, Backhurst *et al.* [1] had two major implications for the metal winning and recovery industries. Firstly batch operation was no longer the only way to proceed and secondly metal in concentrations of a few g.p.l could be processed with excellent efficiencies. The discovery of fluidized bed electrodes (FBE) instigated a number of research programmes into a ‘new generation of cell designs’ for continuous metal reclamation. The main reason for such activity was to improve on the performance of the FBE which had a number of inherent limitations. These included problems of metal deposition on feeder electrodes, bipolar characteristics [2] and poor current efficiencies at current density below 1000 $\mathrm{A\,m^{-2}}$.

A high current efficiency is frequently the key to successful exploitation of any reaction, especially when energy consumption is of utmost concern. This factor alone is therefore a prime performance indicator in comparative studies of cell types with similar geometric configuration. With similar electrolytes, diaphragms and electrode materials, energy consumptions at fixed current densities based on 100% current efficiency would be almost independent of cell design.

Of the particulate electrodes which have evolved from fluidized beds, there are three which utilize a common type of circulating particle motion: (i) the spouted bed electrode (or circulating bed) (SBE) [2]; (ii) the moving bed electrode (MBE) [3]; (iii) the vortex bed electrode (VBE) [4].

The circulating motion tends to produce two regions of solid/liquid flow; a hydraulic conveying region where particulates are transported as a relatively dilute phase and a falling almost packed bed region where solid and liquid flow are countercurrent. The position of feeder electrode(s) and diaphragm determine the type of bed obtained (Fig. 1). This paper considers the operation of the three cell types by making a comparison of performance for a well-documented reaction system, the recovery of heavy metal, e.g. copper from dilute solutions. In addition some hydrodynamic characteristics of circulating beds are described.

2. Experimental details

2.1. *Cells*

Experimental results described in this paper are for the operation of a spouted bed electrode and a moving bed electrode operating in a batch recirculating mode. Details of the MBE are described elsewhere [3], whilst the SBE is shown schematically in Fig. 2. This cell, fabricated in Perspex, is divided into anodic and

0021-891X/88 $03.00 + .12

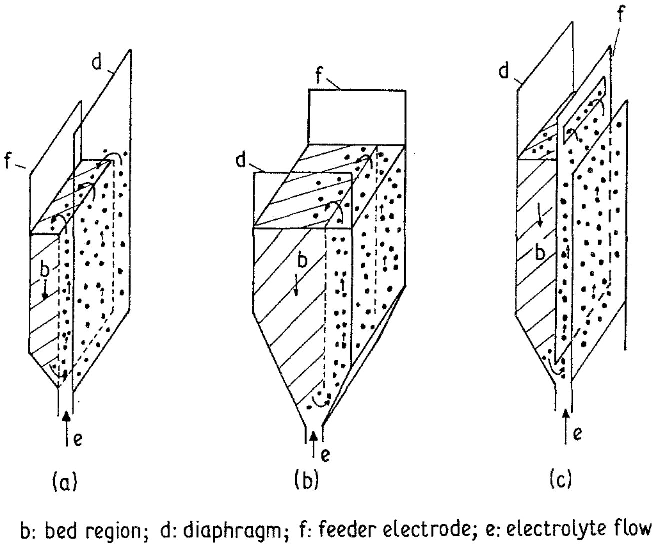

Fig. 1. Schematic diagrams of circulating bed electrodes. (a) Spouted bed; (b) vortex bed; (c) moving bed. b: bed region; d: diaphragm; f: feeder electrode; e: electrolyte flow.

cathodic compartments by a diaphragm. The diaphragm is a cationic exchange membrane Ionac MA 3475, supplied by Ionac Chemical Co. USA. The cathodic compartment, containing the particulate bed, has a thickness of 2.5 cm in the direction of current flow. The cell is tilted during operation to an angle of some 20° to the vertical to aid in particle motion, which is induced by electrolyte flow through a distributor at the base of the cell.

The particulate phase consists of spherical copper particles in the size range 500–700 μm. The cathode feeder is of stainless steel and the anode of platinized titanium. All electrolyses are performed at constant current with power supplied by a Farnell stabilized d.c. supply.

The cell is situated in a dual flow circuit (one for the catholyte, one for the anolyte) consisting of electrolyte holding tanks, recirculating pumps, heat exchangers, flow control valves, filters and flowmeters. All pipework and equipment are made of either PVC, glass reinforced polypropylene or glass. Electrolyte temperatures, pH, cell voltage and charge passed are monitored continuously during each run.

2.2. *Electrolytes*

The catholyte and anolyte are supplied to the cell from separate reservoirs via centrifugal pumps and return by gravitational recycle. The anolyte is a 0.5 M sulphuric acid solution. The catholyte is a copper sulphate solution of approximately 0.016 M ($1\,g\,l^{-1}$ copper) concentration, unless otherwise stated.

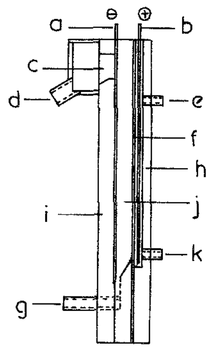

Fig. 2. The experimental spouted bell cell (not to scale). (a) Cathode feeder; (b) anode; (c) weir; (d) catholyte outlet; (e) anolyte outlet; (f) diaphragm support plate; (g) catholyte inlet; (h) analoyte section; (i) cathode section; (j) spouted bed region; (k) anolyte inlet.

In all, three catholyte supporting electrolyte concentrations are used: electrolyte I: 1.0 M sulphuric acid; electrolyte II: 0.1 M sulphuric acid; electrolyte III: no sulphuric acid. The electrolyte copper concentrations, used as the basis on which to determine current efficiencies, are measured by atomic absorption spectrophotometry.

2.3. *Comparative operational basis*

All experiments described in this work are performed using a batch recirculating system under galvanostatic

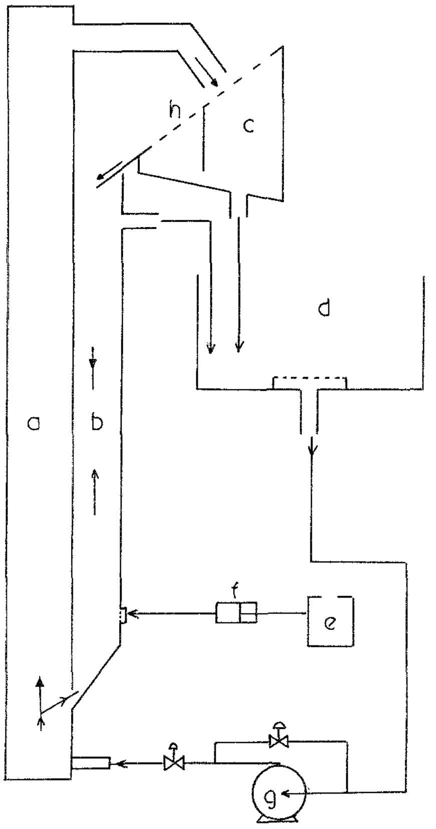

Fig. 3. Hydrodynamic test rig (not to scale). (a) Transport region; (b) moving bed region; (c) solid/liquid separator; (d) water tank; (e) tracer tank; (f) tracer pump; (g) water recirculation pump; (h) screen.

conditions. D.c. power to the cell is supplied via a Farnell stabilized supply and the quantity of charge passed is monitored on a Time Electronics TS 100A digital integrator.

The particulate electrode configuration is such that current flow and electrolyte flow are perpendicular. Current densities quoted in this paper are unless otherwise based on the available diaphragm cross sectional area for current flow.

As a purpose of this work is to compare the operation of three cell types, it is important to ensure that as far as is possible experimental conditions are identical. In this respect the moving bed, spouted bed and vortex bed (described by Stanković and Wragg [4]) are of similar sizes with identical bed widths (2.5 cm) and use a similar copper particle size range. The electrolyte copper concentrations are in all cases approximately $1\,\mathrm{g\,l^{-1}}$.

2.4. *Hydrodynamic test rig*

A schematic diagram of the experimental rig used to study the hydrodynamics of circulating beds is presented in Fig. 3. The circulating bed test section is constructed from Perspex and is approximately 1.5 m high by 0.1 m wide. The thickness of the conveying section and moving bed section are 0.01 m and 0.025 m, respectively. The aperture at the base of the moving bed section can be varied in height by means of an adjustable sliding partition.

Water flow to the test section is from a water tank via a centrifugal pump. On exit from the section the water/solid mixture passes to a screen which enables the solid to be returned to the moving bed and the liquid to the water tank. Water flow through the bed also returns to the water tank. The equipment has provision to measure the overall liquid flow to the test section, the liquid flow through the screen, liquid flow and solid flow along the screen returning to the bed and the liquid overflow from the bed.

The tracer injection system included in the equipment is used to provide visual observation of flow characteristics and to give residence time and liquid velocity data. The tracer used is a solution of potassium permanganate, the concentration of which is readily measured by titration with oxalic acid.

The particulate materials used in this work is glass ballotini beads, 750–1000 μm diameter. Pressure tappings are located at 0.2 m intervals in both the conveying section and moving bed section to enable pressure losses to be measured.

3. Hydrodynamic aspects

The design of the experimental test section to study circulating bed hydrodynamics was chosen because it produced the two well-defined regions of flow, characteristic of such systems. Although data obtained relate directly to the MBE, it is also relevant to both the vortex and spouted beds. In the latter two there is interchange of solid and fluid between the conveying region and bed region. The relative flows of solid and liquid in both regions are controlled, by amongst other things, the overall pressure drop and the aperture size at the base of the bed. It was found that aperture sizes of width either similar to, or greater than, that of the bed induced fluidization. This is obviously not a satisfactory condition for operation; countercurrent flow of solid and liquid is required. The liquid velocity or residence time in the bed is an important parameter in operation; the fraction of flow through this region in relation to the overall flow determines the conversion per pass through an electrode.

The liquid/solid slip (relative) velocity, U_{SL}, in the conveying section is given by [5]

$$e_{\mathrm{c}} U_{\mathrm{SL}} = U_{\mathrm{f}} - e_{\mathrm{r}} U_{\mathrm{s}} = U_{\mathrm{i}} e_{\mathrm{c}}^{n} \qquad (1)$$

where e_{s} is the voidage in this section, U_{f} the superficial liquid velocity, U_{s} the particle velocity, U_{i} the particle terminal velocity, corrected for wall effects, and n is a function of Reynolds number and the ratio of particle size to section cross-section. An equivalent expression to (1) can also be written for the moving bed section

$$V_{\mathrm{f}} = V_{\mathrm{mf}} - e_{\mathrm{b}} V_{\mathrm{s}} \qquad (2)$$

where V_{mf} is the minimum fluidization velocity for the static bed, V_{s} the solid velocity, V_{f} the liquid velocity and e_{b} the bed voidage. A material balance of solid flow between the conveying section and transport line at any cross section is

$$(1 - e_{\mathrm{b}}) V_{\mathrm{s}} S_{\mathrm{b}} = (1 - e_{\mathrm{c}}) U_{\mathrm{S}} S_{\mathrm{T}} \qquad (3)$$

where S_{b} and S_{T} are the cross section of the bed and the conveying sections, respectively.

The fluid flows in the two regions are related through an overall pressure balance

$$\Delta P_{\mathrm{T}} = \Delta P_{\mathrm{b}} \qquad (4)$$

For flow in the conveying section Kopko *et al.* [5] have shown that, for dilute transport of solid in water, the pressure drop is composed of two parts; the static head and solid wall friction losses

$$\frac{\Delta P_{\mathrm{T}}}{L} = (1 - e_{\mathrm{c}})(\varrho_{\mathrm{s}} - \varrho) + \varrho + \frac{2 C_{\mathrm{f}} \varrho \left(\frac{U_{\mathrm{f}}}{e_{\mathrm{c}}} \right)^{2}}{D_{\mathrm{T}}} \qquad (5)$$

where C_{F} is the friction factor, ϱ and ϱ_{s} fluid and solid densities respectively and D_{T} the pipe diameter.

Pressure losses in the moving bed section may be estimated from the work of Yoon and Kunii [6]. They were able to show that for gas/solid flow, the Ergun equation gives reasonable predictions when the slip velocity is used as the correlating velocity.

In principle for a given system the above correlations enable operating characteristics of circulating beds to be determined. In particular solid and liquid velocities in the bed, solid concentration in the conveying section and the fraction of liquid flow in the conveying section.

4. Results

4.1. *Hydrodynamics*

The results of experiments using tracer injection into the test section showed that fluid dispersion effects

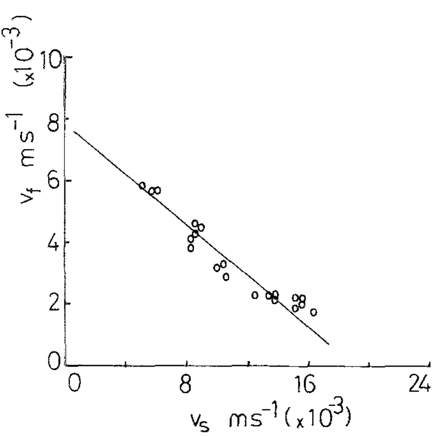

Fig. 4. Correlation of liquid and solid velocities in the moving bed.

were small except at high overall flow rates when the local liquid velocity, V_f, approached zero. The tracer tests also enabled values of V_f to be determined and, hence, comparison with direct measurement. A previous study by Johnson and Turner [7] using ion exchange resins has shown solid motion in countercurrent moving beds to be essentially plug flow.

Experimental correlation of the solid and liquid flows in the moving bed is presented in Fig. 4. The data can be represented in the form

$$V_f = 8 \times 10^{-3} - 0.42\,V_s\,\mathrm{m\,s^{-1}} \qquad (6)$$

The correlated voidage of 0.42 agrees favourably with a value of 0.39 measured for a static bed. The value of $8 \times 10^{-3}\,\mathrm{m\,s^{-1}}$ for the minimum fluidization velocity is in reasonable agreement with a value of $11 \times 10^{-3}\,\mathrm{m\,s^{-1}}$ obtained from the Ergun correlation.

4.1. *Pressure losses*

Typical variations of pressure drop (minus static head) for hydraulic conveying are shown in Fig. 5 as a function of the solid volume percentage $(1 - e_c) \times 100\%$. Pressure losses are clearly greater than those predicted for fluidized beds and agree with the theory of Kopko *et al.* [5].

Measured pressure losses for the moving bed were in the range of 10–12.5 kN m^{-2}. These values agree well with a predicted value of 11.95 kN m^{-2} using the correlation of Happell [8] for a modified friction factor for a moving bed flow

$$C_f = \frac{100}{\mathrm{Re}} + \frac{200}{\mathrm{Re}^{0.2}} \qquad (7)$$

Overall it has been shown that the hydrodynamics of circulating moving beds located in rectangular sections agree well with previous correlations and theory.

4.2. *Electrolysis results*

4.2.1. The spouted bed. The variation of copper ion concentration (electrolyte I) with time obtained with the spouted bed electrode is presented in Fig. 6, for a range of current densities. At high concentrations the depletion rate of copper is approximately linear and tails off as concentrations of 0.2 g l^{-1} are attained. This behaviour is reflected in the equivalent cumulative current efficiency data of Fig. 7, expressed as a function of the dimensionless copper concentration. Current efficiencies fall rapidly at low concentrations.

The influence of current density on current efficiency is shown in Fig. 8. A maximum in current efficiency is clearly exhibited which results from two conflicting effects. At high current densities there is competition between metal deposition and hydrogen evolution whilst at low current densities metal dissolution occurs. The latter effect is more pronounced in electrolytes containing dissolved oxygen. The maximum in

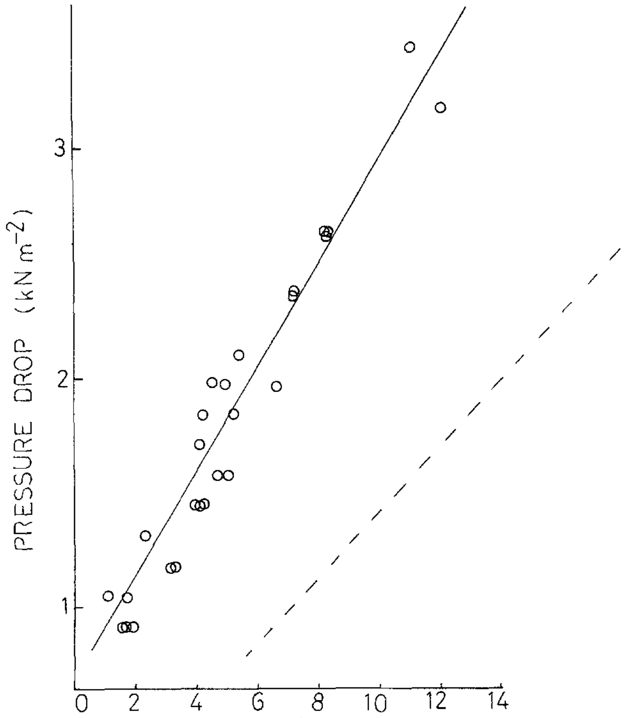

Fig. 5. Correlation of pressure drop in hydraulic conveying: (——) correlation of Kopko [4]; (O) experimental data; (– – –) fluidized bed pressure drop.

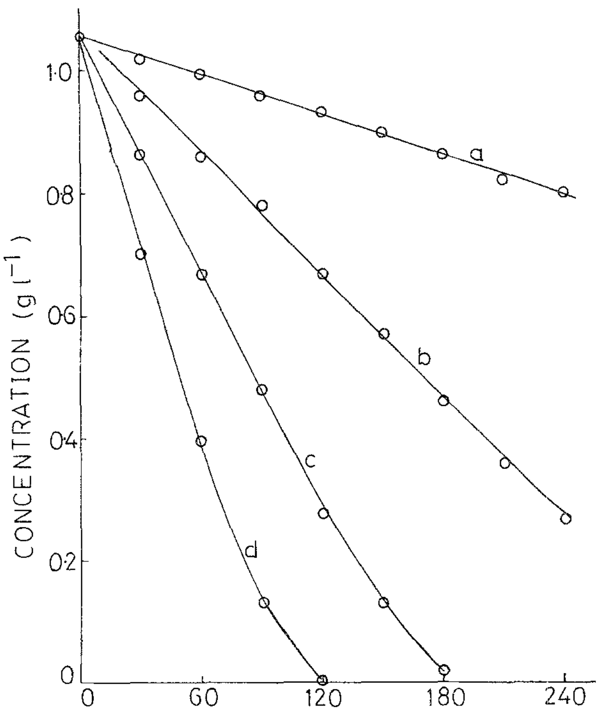

Fig. 6. Concentration–time characteristics of the spouted bed electrode. (a) 300 A m^{-2}; (b) 600 A m^{-2}; (c) 1200 A m^{-2}; (d) 2400 A m^{-2}.

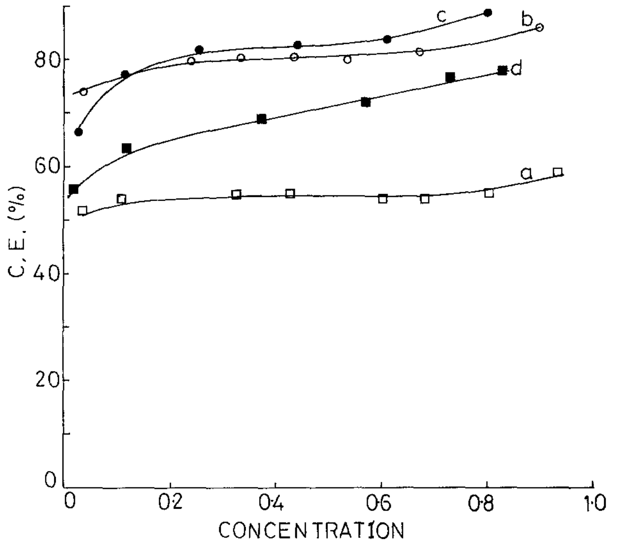

Fig. 7. Variation of mean current efficiency with concentration for the spouted bed electrode. (a) $300\,\mathrm{A\,m^{-2}}$; (b) $600\,\mathrm{A\,m^{-2}}$; (c) $1200\,\mathrm{A\,m^{-2}}$; (d) $2400\,\mathrm{A\,m^{-2}}$.

efficiency is likely to be accentuated by non-uniform potential distributions occurring in the particulate electrode.

There is no mathematical model available which describes the distribution of electrode potential in a circulating bed in which competing reactions occur. Such a model would consist of a 'packed bed' region in parallel with a dissolution/bipolar region with different hydrodynamic characteristics. This however is beyond the scope of the present work.

4.2.2. Comparison of circulating bed electrodes. Concentration–time characteristics. A comparison of the concentration–time characteristics obtained with the VBE and SBE is shown in Fig. 9. The time scale is normalized to $T = It/nFVC_0$, so that a line drawn from $C/C_0 = 1.0$ to $T = 1.0$, corresponds to a current efficiency of 100%. The data for the VBE are from the work of Stanković and Wragg [4] in which current densities are based on the surface area of the particulate bed.

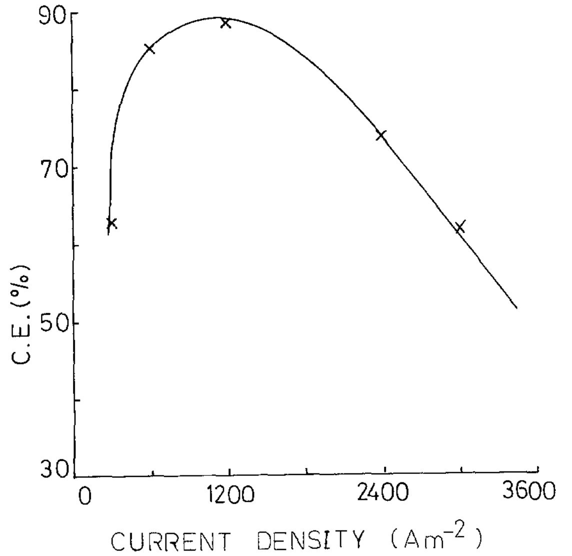

Fig. 8. Variation of mean current efficiency with current density for the spouted bed electrode.

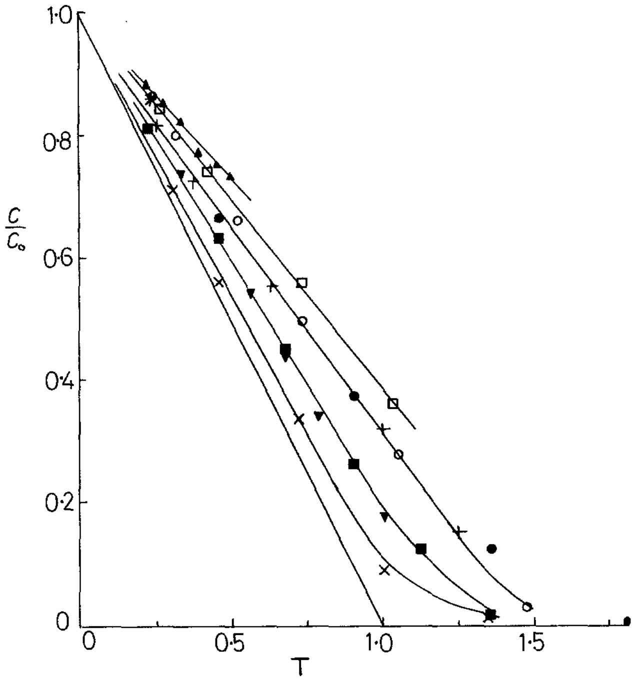

Fig. 9. Comparison of the concentration–time characteristics of the VBE and SBE. Spouted bed: (▲), $300\,\mathrm{A\,m^{-2}}$; (▼), $600\,\mathrm{A\,m^{-2}}$; (■), $1200\,\mathrm{A\,m^{-2}}$; (●), $2400\,\mathrm{A\,m^{-2}}$. Vortex bed [4]: (□), $15\,\mathrm{A\,m^{-2}}$; (○), $18.5\,\mathrm{A\,m^{-2}}$; (+), $22\,\mathrm{A\,m^{-2}}$; (x), $26\,\mathrm{A\,m^{-2}}$.

The behaviour is characteristic of a batch reactor operating at a constant current where initially the depletion of reactant is approximately linear up to a time when the limiting current is reached. After this the concentration decays near exponentially according to the well-known expression for a batch reactor with a diffusion limited reaction

$$C/C_0 = \exp(-K_L at) \tag{8}$$

where K_L is the mass transfer coefficient and a the specific electrode area.

Over the range of conditions considered the SBE and VBE exhibit similar performances. The VBE is also likely to exhibit a maximum in efficiency with current density. This can be appreciated from Fig. 9 knowing that at any concentration, the cumulative current efficiency is given by CE $= C/T \times 100\%$.

4.2.3. Current efficiency. A comparison of differential current efficiencies of the MBE and VBE [4] is presented in Fig. 10. A similarity in performance is once again seen with both electrodes exhibiting relatively poor efficiencies at low concentrations.

The above data from the three particulate electrodes indicate that there is in fact little difference in their performances in the present application of copper recovery. This is not too surprising considering the similarity in the motion of the bed. Mass transfer characteristics of the beds, especially in the 'packed' region responsible for the majority of the metal deposition will be of a similar magnitude. Thus for reaction at or near limiting currents, similar performances are expected. However differences will arise in the distribution of electrode potential in the three electrodes, where for example in the SBE, regions of anodic activity have been identified [9].

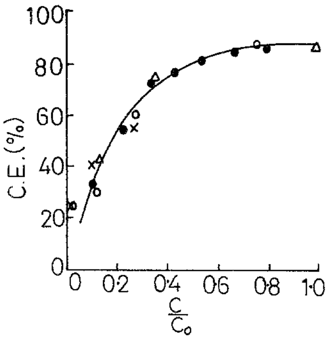

Fig. 10. Comparison of differential current efficiencies of the MBE and VBE [4]. (●), VBE; MBE: (x), 500 A m^{-2}; (△), 1000 A m^{-2}; (○), 1250 A m^{-2}.

4.2.4. *Effect of electrolyte composition.* Process streams and waste waters requiring recovery or removal of toxic metal ions occur with a variety of electrolyte compositions. In particular pH levels can vary significantly from one environment to another. The effect of pH on the performance of circulating bed electrodes is thus investigated, again with reference to copper recovery. Due to the similarity in behaviour of all three electrodes, only one is investigated, the MBE.

The results of a set of runs at different current densities using electrolyte III are shown in Fig. 11. As expected differential current efficiency falls as copper ion concentration decreases, to an extent that at a concentration of 0.1 g l^{-1} current efficiencies are 10% and lower. A significant result is that even at concentrations of 2 g l^{-1} current efficiencies are at best only 70%, which are significantly lower than obtained with electrolyte I. This is believed to be in part due to a non-uniform potential distribution in the bed caused by the low electrolyte conductivity.

The variation of current efficiency with current density is shown in Fig. 12, where as with electrolyte I, a maximum is exhibited. However the range of current density at which current efficiencies are reasonable is small. Experimental results of electrolysis with electrolyte II are also shown in Fig. 12. The general behaviour is similar to that obtained with electrolyte III, although current efficiencies are some 5% lower over the range of current densities used.

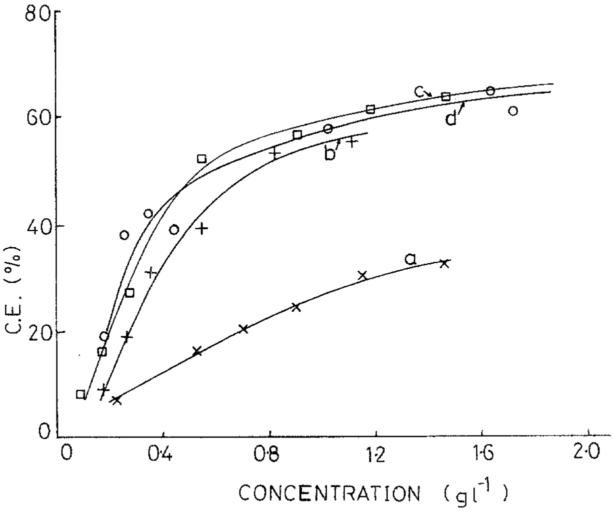

Fig. 11. Current efficiencies for the moving bed. Electrode with high electrolyte pH (electrolyte III): (a) (x), 1500 A m^{-2}; (b) (+), 750 A m^{-2}; (c) (□), 375 A m^{-2}; (d) (○), 187 A m^{-2}.

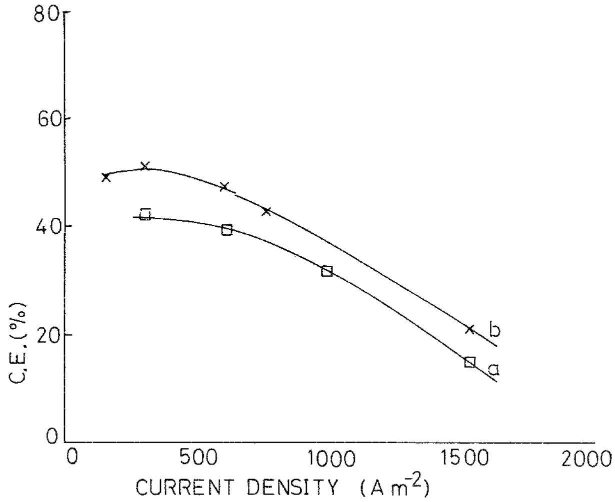

Fig. 12. Variation of current efficiency with current density. (a) Electrolyte II; (b) electrolyte III.

5. Discussion

It has been shown that in the recovery of copper from dilute solutions all three circulating bed electrodes have comparable performances in terms of current efficiency. The recovery of copper is more efficient when electrolyte solutions are of low pH. When only moderately acidic electrolytes are treated, the energy consumption incurs a double penalty in terms of lower current efficiency and a higher cell voltage resulting from the low electrolyte conductivity. The treatment of dilute metal-bearing liquors may therefore benefit from the addition of a low grade acid.

If circulating bed technology were to be adopted for this present type of application, then the selection of the device will be based on other factors such as:

(i) Mode of operation: to induce bed circulation relatively high liquid velocities are required to initiate particle transport. Only a relatively small fraction of the total flow passes through the 'packed bed' region. For example with 500 μm copper particles, estimates of minimum fluidization velocity and minimum transport velocity are 0.0165 m s^{-1} and 0.33 m s^{-1}, respectively. Thus with a ratio of cross-sections of the packed region to conveying region of say 2.5, only 11% of the total flow at a maximum will pass through the packed region. Experimentally measured values are much less than this and hence the degree of reactant conversion per pass is small. In consequence, electrodes will operate with recycle or alternatively be arranged in series-connected banks.

(ii) Pressure drop: all three electrodes considered have similar pressure losses associated with hydraulic transport. These pressure losses are not radically different to those for fluidized beds and as such circulating beds are not too disadvantaged.

(iii) Diaphragm requirement: of the three circulating beds only the SBE can operate without a diaphragm or separator [10] to isolate the conductive bed from the counter electrode.

(iv) Gas evolution: the occurrence of hydrogen evolution in metal deposition reactions is common and has been identified as a contributing factor in the current inefficiency of circulating electrodes. If the rate of gas evolution is relatively high then due to the downward motion of the bed, slugging may occur. This has been observed to some extent in the MBE at high current densities and to a lesser extent in the SBE. A particular problem may arise with slugging if it results in the bed becoming stationary adjacent to the diaphragm. This may then allow metal deposition to occur on the diaphragm with catastrophic consequences. In regard to this problem the SBE will be the preferred electrode owing to the conveying taking place next to the diaphragm.

(v) Scale-up: this factor is of prime importance if adoption of circulating bed technology is to be realized. In flow-by electrodes an increase in scale can only be effectively achieved in the two dimensions associated with the diaphragm or feeder cross-sectional areas. Both the SBE and MBE (with feeder separating the hydraulic conveying and packed region) are amenable to scale-up in this way. This has been demonstrated with beds of approximately 30 cm in length [2, 3] and in the present study with an MBE of 1.5 m in length. The vortex bed's configuration is with conveying and falling bed regions side by side. Experience with a similar configuration of moving bed has shown that on scale-up perpendicular to electrolyte flow, regions of the bed become stationary and susceptible to agglomeration during deposition. The VBE thus appears to have a limited size on scale-up. The factor of scale-up is especially important in circumstances when gas evolution occurs, where pockets or slugs of gas may build-up along the length of the bed. In this respect the SBE is advantaged.

6. Conclusions

The three circulating bed electrodes considered in this work are all potential candidates for the recovery of metals from dilute solutions. All have similar performance characteristics in terms of efficiency of extraction of the metal ion. Of the three, considerations such as scale-up indicate that the SBE has a wider appeal for metal recovery applications.

References

[1] J. R. Backhurst, J. M. Coulson, F. Goodridge and R. E. Plimley, *J. Electrochem. Soc.* **116** (1969) 1600.

[2] F. Goodridge and C. J. Vance, *Electrochim. Acta* **22** (1977) 1073.

[3] K. Scott, *J. Appl. Electrochem.* **11** (1981) 339.

[4] V. D. Stanković and A. A. Wragg, *J. Appl. Electrochem.* **14** (1984) 615.

[5] R. J. Kopko, P. Barton and R. H. McCormick, *Ind. Engng Chem. Proc. Des. Dev.* **14** (1975) 265.

[6] S. M. Yoon and D. Kunii, *Ind. Engng Chem. Proc. Des. Dev.* **9** (1970) 559.

[7] A. S. W. Johnson and J. C. R. Turner, 'Ion-exchange in the Process Industries' Soc. Chem. Ind., London (1969) p. 140.

[8] J. Happell, *Ind. Engng Chem.* **41** (1949) 1161.

[9] F. Coeuret, A. Storck and D. Hutin, *Entropie* **104** (1982) 57.

[10] F. Goodridge and K. Scott, *J. Appl. Electrochem.* **11** (1981) 723.